Recursive density-matrix-spectral-moment algorithm for molecular nonlinear polarizabilities

Sergei Tretiak, Vladimir Chernyak, and Shaul Mukamel
Department of Chemistry, University of Rochester, Rochester, New York 14627

(Received 18 July 1996; accepted 6 August 1996)

An iterative algorithm is developed for calculating nonlinear optical polarizabilities using a series of generalized sum rules that resemble the Lanczos algorithm and connect spectral moments of the driven single-electron density matrix to ground state charge distributions and bonding network. The size scaling and saturation of off-resonant polarizabilities (up to seventh order) of polyacetylene oligomers with up to 300 carbon atoms is analyzed in terms of collective electronic oscillators. Simple analytical expressions for size and bond-length alternation dependence of off-resonant polarizabilities are derived using a single-oscillator approximation. © *1996 American Institute of Physics.* [S0021-9606(96)02542-1]

I. INTRODUCTION

Relations between chemical and electronic structure and linear and nonlinear optical polarizabilities of conjugated molecule have drawn much attention of chemists and physicists over the past 20 years.[1–4] Resonant nonlinear spectroscopy provides most valuable information on states that are not accessible by linear techniques,[5–9] whereas off-resonant measurements probe the collective response of many molecular eigenstates.[1–3]

The size scaling of various optical properties has been studied extensively, both theoretically[10–12] and experimentally.[5,9,13,14] Linear absorption of short oligomers with $N<12-20$ carbon atoms shows an $\Omega\sim N^{-\mu}$ scaling of the optical gap with $\mu\sim 0.4–0.6$.[5] The Hückel model yields $\mu=1$.[12] An important relation is the scaling of nonlinear susceptibilities with molecular size. The power scaling law $\gamma\sim N^{b}$ for the third-order polarizability, where N is the number of carbon atoms, has been established experimentally in the early 70s,[15] and supported by theoretical calculations using the free electron model.[16] Numerous subsequent studies showed that for short chains, the exponent b can vary between 3 and 8, depending on the system and model, and eventually approaches 1 (saturates) for long molecules. The crossover between these two behaviors is related to the exciton coherence size.[4,5,13] Calculations performed using the Hückel model (which neglects Coulomb interactions) predict saturation at long chains ($N\sim 50$) and $b\sim 5-9$,[12,17] whereas calculations based on the Pariser–Parr–Pople (PPP) Hamiltonian, which includes electronic correlations, predict a shorter saturation size ($N\sim 20-30$) and $b\sim 4-5$.[1,4,18] Sum-over-states calculations of γ in short oligomers yield a scaling exponents $b\approx 8$ for symmetric linear cyanites and $b\approx 4$ for linear polyenes.[19] Difficulties with the controlled synthesis and poor solubility of polyenic oligomers restricted early experimental studies to molecules with up to 30–40 carbon atoms,[14,15,20] which showed no saturation. These problems have been overcome, and the saturation of γ has been observed experimentally at ~200 double bonds,[13] which is much larger than early estimates.

Considerable attention has been also paid to the dependencies of nonlinearities on other molecular parameters. It has been argued that the bond-length alternation parameter Δ is related to electron localization.[21] In alternating chains the Hückel model predicts $\gamma\sim\Delta^{-6}$ divergence at small Δ.[12] Flytzanis and co-workers employed the Hückel model to study the scaling of off-resonant γ of large oligomers with the saturated optical gap $\widetilde{\Omega}$.[10,21] The resulting $\gamma\sim\widetilde{\Omega}^{-6}$ scaling law is in qualitative good agreement with experimental data collected for both off-resonant and resonant third-order polarizabilities of different conjugated polymers.[22] Recent resonant experiments show the following relation $\gamma(-3\omega;\omega,\omega,\omega)/\alpha_{\max}\sim\widetilde{\Omega}^{-10}$ (Refs. 5 and 9), where the scaling of both γ and $\alpha_{\max}$ (absorption maximum) depends on the concentration of chromophores in films, and the ratio is approximately independent on dilution.

Calculations of optical hyperpolarizabilities usually involve an extensive numerical effort. The sum-over-states (SOS)[3,23] method includes the calculations of both the ground state and excited states wave functions and the transition dipole moments between them. The time-dependent Hartree–Fock (TDHF) procedure[4,24–26] which is based on the solution of equations of motion for the single-electron reduced density matrix,[27] provides an oscillator (quasiparticle) picture of the optical response.[4,24] This allows the description of electronic motions in terms of collective electronic normal modes, in complete analogy with the standard treatment of nuclear vibrations. Within this approximation, the only relevant ground state information is the Hartree–Fock (HF) ground state reduced single-electron density matrix, whose diagonal elements give electronic charges, and the off-diagonal elements characterize the bond order.[27] Important interference effects are naturally built in, and it reproduces the correct scaling with system size. The TDHF has tremendous computational advantages over the sum-over-states method, but calculating the oscillators still requires the diagonalization of a $K^2\times K^2$ matrix representing the linearized TDHF equations, K being the basis set size. Even though it has been established that only a few oscillators eventually dominate the response, we cannot tell that beforehand. We then need to first calculate all the oscillators and

 0021-9606/96/105(19)/8914/15/$10.00

then sort them out to find the dominant ones. This poses a severe computational problem since we end up calculating much redundant information. The TDHF is a great improvement over the sum over states; however, sorting out the oscillators is still a major difficulty.

In this paper we develop a simple and extremely powerful density-matrix-spectral-moment algorithm (DSMA) for calculating linear and nonlinear optical response of a many-electron system. The method allows us to focus on the relevant oscillators from the outset, thus greatly reducing computational cost and clearly establishing the origin of the dominant mode picture. This is accomplished using a family of sum rules which connect the short-time behavior of the response function of many-electron systems to ground state properties. By applying the closed expressions derived in Ref. 28, we can then calculate the frequency-dependent optical susceptibilities using a small number of parameters characterizing the dominant modes. The short-time response functions are determined by these parameters as well. By solving these equations and substituting the parameters into the expressions for the polarizabilities, we establish a connection between the polarizabilities and the ground state reduced single-electron density matrix.

The DSMA has a close formal connection with other short-time algorithms widely used in different contexts. These include the Lanczos algorithm for computing the eigenvalues of a hermitian matrix,[29] the Mori–Zwanzig procedure of reduced dynamics,[30] and the continued fraction representation of correlation functions.[31] In particular, we note the analogy with the analysis of optical line shapes in terms of spectral moments.[32] The moments can be easily calculated without going through a complex eigenvalue problem, and often very few moments provide for an adequate representation of the line shape. We use the same ideas to compute nonlinear optical susceptibilities. We calculate the spectral moments of the density matrix induced by the external field, and use them to construct the electronic modes relevant to the optical response. Similar to conventional moment analysis, convergence is verified by incrementally adding more moments.

In Sec. II we introduce the tight-binding Hamiltonian for π electrons and present the restricted TDHF equation[4,24] which describes the time evolution of particle–hole (interband) components of the reduced single-electron density matrix ρ. In Appendix A we show how to express the intraband components of ρ in terms of the interband part ξ of the deviation of ρ from its ground state $\overline{\rho}$. In Sec. III we express the polarization using the eigenmodes ξ_ν of the linearized TDHF equation. The DSMA which makes it possible to calculate polarizabilities at any order, keeping as many modes as necessary, is presented in Sec. IV. The relations necessary for numerical applications of the DSMA are outlined in Appendix B. In Sec. V we present numerical calculations for polyacetylene oligomers and discuss the computational advantages of the DSMA. We further give a simple analytical expression for off-resonant polarizabilities obtained using a crude single-oscillator approximation. The detailed derivations of this formula are given in Appendices C, D, and E. This expression is in excellent agreement with the full TDHF calculations, reproduces the correct scaling of observables, and provides a simple and clear physical connection between chemical and optical properties.

II. THE TIGHT-BINDING HAMILTONIAN AND THE SINGLE-ELECTRON DENSITY MATRIX

We consider a π-electron system described by the tight-binding Pariser–Parr–Pople (PPP) Hamiltonian which reproduces many important properties of conjugated polyenes[33]

$$\hat{H}=\sum_{m,n,\sigma} t_{mn}c^{+}_{m,\sigma}c_{n,\sigma}+\tfrac{1}{2}\sum_{m,n,\sigma,\sigma'} V_{nm}c^{+}_{m,\sigma} \times c^{+}_{n,\sigma'}c_{n,\sigma'}c_{m,\sigma}-\mathscr{E}(t)\sum_{n,\sigma}\mu_{nn}c^{+}_{n,\sigma}c_{n,\sigma}, \tag{1}$$

where $c^{+}_{m,\sigma}(c_{m,\sigma})$ is the annihilation (creation) operator of a π electron on site m with spin σ, satisfying the Fermi anticommutation relation $\{c^{+}_{m,\sigma},c_{n,\sigma'}\}=\delta_{m,n}\delta_{\sigma,\sigma'}$.

The first term is the Hückel hamiltonian, where $t_{nn}=\Sigma_m V_{nm}$ is the Coulomb integral at the nth atom and t_{mn} $(m\neq n)$ is the nearest-neighbor transfer integral between the nth and mth atoms: $t_{n,n\pm1}=\beta-\beta' l_n$ and l_n is the deviation of the nth bond length from the mean bond length along the chain. The second term represents electron–electron Coulomb interactions; the repulsion between the nth and mth sites is given by Ohno's formula

$$V_{nm}=\frac{U}{\sqrt{1+(r_{nm}/a_0)^2}}, \tag{2}$$

where $U=U_0/\epsilon$ is the on-site Hubbard repulsion and ϵ is the static dielectric constant. The last term represents interaction between π electrons and an external field $\mathscr{E}(\mathbf{t})$ polarized along the chain z axis. We assume a localized basis set so that the dipole moment is diagonal $\mu_{nm}=ez_n\delta_{nm}$. The size of the basis set is equal to the number of carbon atoms $K=N$. The parameters used were adjusted to reproduce the energy gap for polyacetylene (2.0 eV): $U_0=11.13$ eV, $\beta=-2.4$ eV, $\beta'=-3.0$ eV Å^{-1}, $\epsilon=1.5$, $a_0=1.2935$ Å.[4] In all calculations we used fixed geometry with unit cell size along the backbone $a=1.22$ Å and bond-length alternation parameter $l_n=\Delta=0.07$ Å.

Analysis of our paper is based on following the evolution of the reduced single-electron density matrix

$$\rho^{\sigma}_{nm}(t)=\langle\Psi(t)|c^{+}_{m,\sigma}c_{n,\sigma}|\Psi(t)\rangle, \tag{3}$$

where $\Psi(t)$ is the time-dependent many-electron wave function. In the present model the wave function is a singlet at all times, so that spin variables may be eliminated.[24] We first find the ground state HF single-electron density matrix $\overline{\rho_{nm}}$ by solving the stationary HF equation using iterative diagonalization[4]

$$[h(\overline{\rho}),\overline{\rho}]=0. \tag{4}$$

Here h is the Fock operator

$$h(\overline{\rho})=t+V(\overline{\rho}), \tag{5}$$

and $V(\overline{\rho})$ is the Coulomb operator

$$V(\overline{\rho})_{mn} = -V_{mn}\overline{\rho_{mn}} + 2\delta_{mn}\sum_l V_{ml}\overline{\rho_{ll}}. \tag{6}$$

When the molecule is driven by an external field, the density matrix acquires a time-dependent part $\delta\rho(t)$ and we have

$$\rho(t) = \overline{\rho} + \delta\rho(t) = \overline{\rho} + \xi(t) + T(\xi(t)). \tag{7}$$

Here ξ represents the particle–hole (interband) and $T(\xi)$ is the particle–particle and the hole–hole (intraband) parts of $\delta\rho(t)$. The matrix $T(\xi(t))$ is given by the following expansion, which can be derived using the relation $\rho(t)^2 = \rho(t)$ (see Appendix A)

$$T(\xi) = \left(\overline{\rho} - \frac{I}{2}\right)(I - \sqrt{I - 4\xi^2}), \tag{8}$$

where I is the unit matrix. Equation (8) can be expanded in powers of ξ

$$T(\xi) = (I - 2\overline{\rho})(\xi^2 + \xi^4 + 2\xi^6 + \cdots), \tag{9}$$

or alternatively (see Appendix A)

$$T(\xi) = \frac{1}{2!}[[\xi,\overline{\rho}],\xi] + \frac{1}{4!}[[\xi,\overline{\rho}],[[\xi,\overline{\rho}],[[\xi,\overline{\rho}],\xi]]] + \cdots. \tag{10}$$

In Eqs. (9) and (10), all ξ are taken at time t, $\xi = \xi(t)$. Expansions (9) and (10) are identical. For example, to second order in ξ, Eq. (10) reads $\frac{1}{2!}[[\xi,\overline{\rho}],\xi] = \xi\overline{\rho}\xi - \frac{1}{2}(\overline{\rho}\xi^2 + \xi^2\overline{\rho})$. The projection property of $\overline{\rho}$ (Ref. 24) implies the following relations for any interband density matrix ξ: $\xi = \overline{\rho}\xi + \xi\overline{\rho}$ and $\overline{\rho}\xi^2 = \xi^2\overline{\rho}$ (note, that ξ^2 is an intraband matrix). Using these identities we recover the second-order term in Eq. (9).

The evolution of the reduced density matrix is described by the time-dependent Hartree–Fock (TDHF) equation

$$i\frac{\partial\xi}{\partial t} = L\xi - \mathscr{E}[\mu,\overline{\rho}] + [[R(\xi),\overline{\rho}],\overline{\rho}], \tag{11}$$

whose linear part is

$$L\xi = [t + V(\overline{\rho}),\xi] + [V(\xi),\overline{\rho}]. \tag{12}$$

L is a linear operator in Liouville space (i.e., superoperator)[4] and

$$R(\xi) = [V(\xi),\xi] + [V(T(\xi)),\xi] + [V(T(\xi)),\overline{\rho}] + [V(\xi),T(\xi)] - \mathscr{E}[\mu,\xi + T(\xi)]. \tag{13}$$

$R(\xi)$ contains both inter- and intraband components, and the projection property of $\overline{\rho}$ (Ref. 24) is used to project $R(\xi)$ onto the particle–hole subspace $R_{p-h} = [[R(\xi),\overline{\rho}],\overline{\rho}]$.

The time-dependent polarization, which determines all optical properties, is finally given by

$$P(t) = \mathrm{Tr}(\mu\xi(t)) + \mathrm{Tr}(\mu T(t)), \tag{14}$$

where $T(t) \equiv T(\xi(t))$, and the dipole operator is represented by a diagonal matrix with elements $\mu_{nm} = ez_n\delta_{nm}$. (Note that the trace includes summation over spin variables. For a given spinless system[24] it is twice the trace over space variables.)

III. THE NONLINEAR OPTICAL RESPONSE AND ELECTRONIC NORMAL MODES

The equations of motion (11) may be solved by expanding the interband (particle–hole) components of the reduced single-electron density matrix in powers of the external field

$$\xi = \xi^{(1)} + \xi^{(2)} + \xi^{(3)} + \cdots. \tag{15a}$$

The intraband (particle–particle and hole–hole) components are similarly given by

$$T(\xi) = T^{(2)}(\xi) + T^{(3)}(\xi) + T^{(4)}(\xi) + \cdots, \tag{15b}$$

where $T^{(j)}(t)$ is expressed in terms of $\xi^{(j)}$ by comparing Eq. (9) [or Eq. (10)] with the Eqs. (15). $T^{(1)}(t) \equiv 0$, $T^{(2)}(t) = (I - 2\overline{\rho})[\xi^{(1)}(t)]^2$, etc. Polarization to the jth order in the external field $\mathscr{E}(t)$ is calculated by taking the expectation value of the dipole operator μ with respect to the time-dependent density matrix

$$P^{(j)}(t) = \mathrm{Tr}(\mu\,\delta\rho^{(j)}(t)), \tag{16}$$

with

$$\delta\rho^{(j)}(t) = \xi^{(j)}(t) + T^{(j)}(t). \tag{17}$$

Using these equations, the original nonlinear equation (11) is transformed into a hierarchy of linear inhomogeneous equations. To jth order we have

$$i\frac{\partial\xi^{(j)}(t)}{\partial t} - L\xi^{(j)}(t) = \eta^{(j)}(t). \tag{18}$$

The formal solution of this equation in the frequency domain is

$$\xi^{(j)}(\omega) = \mathscr{G}_0(\omega)\,\eta^{(j)}(\omega), \tag{19}$$

where

$$\mathscr{G}_0(\omega) = \frac{1}{\omega - L}, \tag{20}$$

is a zero-order tetradic Green function, and $\eta^{(j)}(t)$ is jth-order term from the right-hand side of Eq. (11) $\eta^{(1)}(t) = -\mathscr{E}(t)[\mu,\overline{\rho}]$, etc. Throughout this paper, the Fourier transform is defined by

$$f(\omega) = \int_{-\infty}^{\infty} dt e^{i\omega t} f(t). \tag{21}$$

The optical polarizabilities are readily obtained using $\delta\rho^{(j)}(\omega)$. Following the procedure outlined in Appendix D of Ref. 4, $\eta^{(j)}(\omega)$, $T^{(j)}(\omega)$, and $\xi^{(j)}(\omega)$ contain permutations over all frequencies of the applied fields, which are given by

$$\mathscr{E}(t) = \sum_k \mathscr{E}_0^{(k)} \cos\,\omega_k t. \tag{22}$$

The jth order frequency-dependent polarization is

$$P^{(j)}(\mp\omega_1\mp\cdots\mp\omega_j;\pm\omega_1,\ldots,\pm\omega_j)$$
$$=\chi^{(j)}(\mp\omega_1\mp\cdots\mp\omega_j;\pm\omega_1,\ldots,\pm\omega_j)\mathscr{E}_0^{(1)}\cdots\mathscr{E}_0^{(j)}, \quad (23)$$

and the optical polarizabilities assume the form

$$\chi^{(j)}(\mp\omega_1\mp\cdots\mp\omega_j;\pm\omega_1,\ldots,\pm\omega_j)$$
$$=-\frac{1}{\mathscr{E}_0^{(1)}\cdots\mathscr{E}_0^{(j)}}\,\mathrm{Tr}(\mu\,\delta\rho^{(j)}(\mp\omega_1\mp\cdots\mp\omega_j;\pm\omega_1,\ldots,\pm\omega_j)). \quad (24)$$

Hereafter we focus on the off-resonant response. Setting all frequencies to zero, we obtain

$$\begin{aligned}
&T^{(1)}(\omega=0)\equiv 0,\\
&T^{(2)}(\omega=0)=(I-2\overline{\rho})(\xi^{(1)})^2,\\
&T^{(3)}(\omega=0)=(I-2\overline{\rho})(\xi^{(2)}\xi^{(1)}+\xi^{(1)}\xi^{(2)}),\\
&T^{(4)}(\omega=0)=(I-2\overline{\rho})(\xi^{(3)}\xi^{(1)}+\xi^{(2)}\xi^{(2)}+\xi^{(1)}\xi^{(3)}),
\end{aligned} \quad (25)$$

and

$$\begin{aligned}
&\eta^{(1)}(\omega=0)=-\mathscr{E}_0[\mu,\overline{\rho}],\\
&\eta^{(2)}(\omega=0)=[[([V(\delta\rho^{(1)}),\delta\rho^{(1)}]+[V(T^{(2)}),\overline{\rho}]\\
&\qquad -\mathscr{E}_0[\mu,\delta\rho^{(1)}]),\overline{\rho}],\overline{\rho}],\\
&\eta^{(3)}(\omega=0)=[[([V(\delta\rho^{(2)}),\delta\rho^{(1)}]+[V(\delta\rho^{(1)}),\delta\rho^{(2)}]\\
&\qquad +[V(T^{(3)}),\overline{\rho}]-\mathscr{E}_0[\mu,\delta\rho^{(2)}]),\overline{\rho}],\overline{\rho}].
\end{aligned} \quad (26)$$

Here $\xi^{(j)}\equiv\xi^{(j)}(\omega=0)$ and $\delta\rho^{(j)}\equiv\delta\rho^{(j)}(\omega=0)$. The off-resonant polarizabilities are given by

$$\chi^{(j)}=-\frac{1}{\mathscr{E}_0^j}\,(\mathrm{Tr}(\mu\xi^{(j)}(\omega=0))+\mathrm{Tr}(\mu T^{(j)}(\omega=0))), \quad (27)$$

where $\chi^{(1)}$, $\chi^{(3)}$, $\chi^{(5)}$ denote the polarizabilities α, γ, δ, etc.

To compute Eqs. (19) we need to find all eigenmodes ξ_ν and eigenfrequencies Ω_ν of the Liouville operator L,[4]

$$L\xi_\nu=\Omega_\nu\xi_\nu. \quad (28)$$

The eigenmodes come in pairs: Each vector ξ_ν with frequency Ω_ν has a counterpart $\xi_{-\nu}=\xi_\nu^+$ with frequency $-\Omega_\nu$. Since L is real, the electronic modes can be taken to be real. We shall adopt the following normalization for the eigenvectors related to positive frequencies[24]

$$\mathrm{Tr}(\overline{\rho}[\xi_\alpha^+,\xi_\beta])=\delta_{\alpha\beta}, \quad (29a)$$

$$\mathrm{Tr}(\overline{\rho}[\xi_\alpha^+,\xi_\beta^+])=\mathrm{Tr}(\overline{\rho}[\xi_\alpha,\xi_\beta])=0. \quad (29b)$$

Using these modes, the Green function assumes the form

$$\mathscr{G}_0(\omega)=\sum_\nu\frac{\xi_\nu^+\xi_\nu}{\omega-\Omega_\nu}, \quad (30)$$

where we used a tensor notation, and the sum runs over all modes with positive as well as negative frequencies.

A classical mode picture of optical response is obtained by constructing the electronic oscillators defined by the coordinate-momentum variables

$$Q_\nu=\frac{\xi_\nu+\xi_\nu^+}{\sqrt{2}},\quad P_\nu=-i\,\frac{\xi_\nu-\xi_\nu^+}{\sqrt{2}}. \quad (31)$$

The normalization of Q_ν and P_ν follows directly from Eqs. (29)

$$\mathrm{Tr}(\overline{\rho}[P_\alpha,Q_\beta])=i\,\delta_{\alpha\beta}, \quad (32a)$$

$$\mathrm{Tr}(\overline{\rho}[P_\alpha,P_\beta])=\mathrm{Tr}(\overline{\rho}[Q_\alpha,Q_\beta])=0. \quad (32b)$$

The linearized TDHF equation thus reads $\dot{Q}_\nu=-\Omega_\nu P_\nu$, $\dot{P}_\nu=\Omega_\nu Q_\nu$.

The coupled electronic oscillator representation maps the calculation of the optical response onto the dynamics of a set of anharmonic oscillators representing the electron–hole pair components of the reduced single-electron density matrix. The linear polarizability then assumes the form[24]

$$\chi^{(1)}(\omega)=\sum_{\nu=1}^{N^2/4}\frac{\Omega_\nu[\mathrm{Tr}(\mu Q_\nu)]^2}{\Omega_\nu^2-(\omega+i\epsilon)^2}, \quad (33)$$

where ϵ is a linewidth. Closed expressions for $\chi^{(2)}$ and $\chi^{(3)}$ were given in Ref. 24.

Calculating the electronic modes is the most computationally demanding task of the TDHF scheme, since we retain the complete information about the single-electron density matrix. The procedure becomes numerically intractable for long chains. Applications of the procedure have been limited to $N\sim 40$ atoms. The DSMA developed in the next section overcomes this difficulty.

IV. THE DENSITY-MATRIX-SPECTRAL-MOMENT ALGORITHM

The DSMA allows us to calculate $\xi^{(j)}$ from $\eta^{(j)}$ by solving Eq. (19) without a direct diagonalization of L. In principle we need to expand the interband components $\xi^{(j)}$ of the reduced single-electron density matrix in the complete set of eigenmodes of L. Typically, however, only a few modes (4–5) contribute to the response.[34] The DSMA reduces the computational effort considerably by calculating only these relevant modes.

The interband component of the reduced single-electron density matrix to jth order in the field $\xi^{(j)}(\omega)$ [Eq. (19)] can be represented as

$$\xi^{(j)}(\omega)=\int_0^{+\infty}dt e^{i\omega t}S^{(j)}(t,\omega), \quad (34)$$

where we have introduced the matrix $S^{(j)}(t,\omega)$

$$S^{(j)}(t,\omega)\equiv -ie^{-iLt}\eta^{(j)}(\omega). \quad (35)$$

This matrix satisfies the equation

$$i\,\frac{\partial S^{(j)}(t,\omega)}{\partial t}-LS^{(j)}(t,\omega)=0, \quad (36)$$

with the initial condition

$$S^{(j)}(0,\omega)=-i\,\eta^{(j)}(\omega). \quad (37)$$

In Eqs. (35) and (37) the $S^{(j)}$ matrix is viewed as a vector in Liouville space. We next expand the solution of Eq. (36) in a Taylor series

$$S^{(j)}(t,\omega)=-i\left(S_0^{(j)}(\omega)+(-i)\,\frac{S_1^{(j)}(\omega)}{1!}\,t+\cdots\right)$$

$$=-i\sum_{n=0}\,(-i)^n\,\frac{S_n^{(j)}(\omega)}{n!}\,t^n, \tag{38}$$

where $S_0^{(j)}(\omega)=\eta^{(j)}(\omega)$ and $S_k^{(j)}(\omega)=L^kS_0^{(j)}(\omega)$, $k=1,2,\ldots$. This expansion, which describes the short-time evolution of initial vector $\eta(\omega)$ in the subspace determined by $-ie^{-iLt}$, allows us to calculate $S_{k+1}^{(j)}$ recursively

$$S_{k+1}^{(j)}=LS_k^{(j)}=[t+V(\overline{\rho}),S_k^{(j)}]+[V(S_k^{(j)}),\overline{\rho}]. \tag{39}$$

Since the procedure involves merely matrix multiplication (no inversion or diagonalization), it can be readily applied even for very large systems (thousands of atoms).

We will use the short-time expansion (38) to derive an algorithm for computing the electronic normal modes. $\eta^{(j)}(\omega)$ can be expressed in terms of the modes [Eq. (4.16a) in Ref. 24]

$$\eta^{(j)}(\omega)=\sum_{\nu=1}^{N^2/4}\,(\mathrm{Tr}(\overline{\rho[}\xi_\nu^+,\eta^{(j)}(\omega)])\xi_\nu$$

$$-\mathrm{Tr}(\overline{\rho[}\xi_\nu,\eta^{(j)}(\omega)])\xi_\nu^+). \tag{40}$$

Using the mode representation, the solution of Eq. (36) can be written as

$$S^{(j)}(t,\omega)=-i\sum_{\nu=1}^{N^2/4}\,(\mathrm{Tr}(\overline{\rho[}\xi_\nu^+,\eta^{(j)}(\omega)])\xi_\nu\,\exp(-i\Omega_\nu t)$$

$$-\mathrm{Tr}(\overline{\rho[}\xi_\nu,\eta^{(j)}(\omega)])\xi_\nu^+\,\exp(i\Omega_\nu t)). \tag{41}$$

Since the electronic modes are real, the expansion coefficients can be taken to be real and we have

$$\mathrm{Tr}(\overline{\rho[}\xi_\nu^+,\eta^{(j)}(\omega)])=\mathrm{Tr}(\overline{\rho[}\xi_\nu,\eta^{(j)}(\omega)])$$

$$=\mathrm{Tr}(\mu^{(j)}(\omega)\xi_\nu^+)\equiv\frac{\mu_\nu^{(j)}(\omega)}{\sqrt{2}}, \tag{42}$$

and

$$\mathrm{Tr}(\mu^{(j)}(\omega)Q_\nu)\equiv\mu_\nu^{(j)}(\omega),\quad \mathrm{Tr}(\mu^{(j)}(\omega)P_\nu)\equiv 0, \tag{43}$$

where we have introduced the effective dipole moment for the jth-order nonlinear response $\mu^{(j)}(\omega)$, using the projection property of $\overline{\rho}$

$$\mu^{(j)}(\omega)=[\eta^{(j)}(\omega),\overline{\rho}],\quad \eta^{(j)}(\omega)=[\mu^{(j)}(\omega),\overline{\rho}]. \tag{44}$$

In particular, for the linear response we have $\mu^{(1)}(\omega)=-\mathscr{E}(\omega)\mu$.

Making use of the oscillator coordinates and momenta [Eq. (31)], we can finally recast Eq. (41) in terms of normal modes

$$S^{(j)}(t,\omega)=\sum_{\nu=1}^{N^2/4}\,\mu_\nu^{(j)}(\omega)[Q_\nu\,\sin(\Omega_\nu t)+P_\nu\,\cos(\Omega_\nu t)]. \tag{45}$$

The jth-order interband component of the reduced single-electron density matrix can be expanded in the form

$$\xi^{(j)}(\omega)=\sum_{\nu=1}^{N^2/4}\,\mu_\nu^{(j)}(\omega)\left[\frac{\Omega_\nu}{\Omega_\nu^2-\omega^2}\,Q_\nu-\frac{i\omega}{\Omega_\nu^2-\omega^2}\,P_\nu\right]. \tag{46}$$

This resembles the response of a collection of electronic oscillators with frequencies Ω_ν and effective (frequency-dependent) transition dipoles $\mu_\nu^{(j)}(\omega)$.

To find the normal coordinates and momenta, we expand the cos and the sin functions in a Taylor series, and compare coefficients of the same powers of t with Eq. (38). This yields

$$S_n^{(j)}(\omega)=i\sum_{\nu=1}^{M}\,\Omega_\nu^n\mu_\nu^{(j)}(\omega)P_\nu,\quad n=0,2,4,\ldots,2M-2, \tag{47a}$$

$$S_n^{(j)}(\omega)=\sum_{\nu=1}^{M}\,\Omega_\nu^n\mu_\nu^{(j)}(\omega)Q_\nu,\quad n=1,3,5,\ldots,2M-1. \tag{47b}$$

These are closed equations for $2M$ parameters (μ_ν,Ω_ν), and $2M$ $N\times N$ matrices (P_ν and Q_ν). M is the desired number of modes which can be controlled by the number of moments we keep, $M=1,2,\ldots$.

Using identity (44), we can trace these equations with the effective dipole moment, resulting in a nonlinear system of $2M$ equations for the M frequencies Ω_ν and M effective oscillator strengths $f_\nu^{(j)}(\omega)\equiv\Omega_\nu(\mu_\nu^{(j)}(\omega))^2$

$$\sum_{\nu=1}^{M}\,f_\nu^{(j)}(\omega)\Omega_\nu^{2k}=K_k^{(j)}(\omega),\quad k=0,1,2,\ldots,2M-1, \tag{48}$$

where

$$K_k^{(j)}(\omega)\equiv\mathrm{Tr}(\mu^{(j)}(\omega)S_{2k+1}^{(j)}(\omega)), \tag{49}$$

are the even spectral moments of jth-order nonlinear polarizability. Equations (49) and (39) provide an extremely convenient algorithm of computing the higher-order spectral moments. Alternative expressions for the spectral moments, which provide a better physical insight, since they highlight the crucial role of the bond alternation in the spectral moments, are given in Appendix C. However, Eqs. (49) and (39) are more suitable for numerical computations.

The system (48) can be easily solved numerically for $f_\nu^{(j)}(\omega)$ and Ω_ν, as shown in Appendix B. This results in the dominant mode frequencies and their oscillator strengths. We start with a single mode approximation, and by successively adding new modes we obtain improved approximations for frequencies and oscillator strengths of the dominant modes, until some convergence criteria are satisfied. At each level of the hierarchy (determined by M) the resulting oscil-

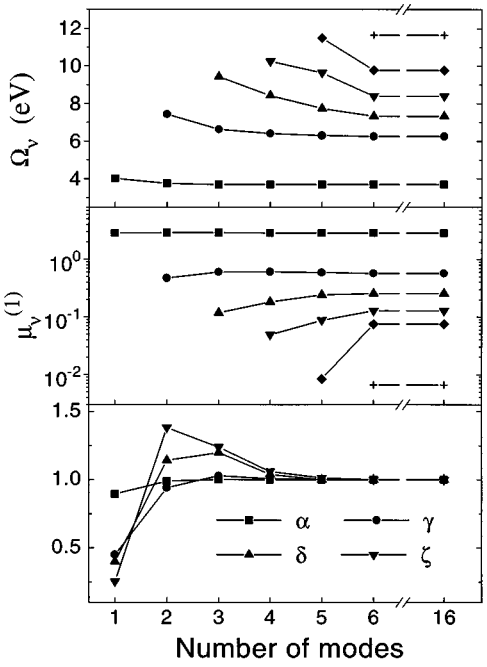

FIG. 1. Variation of electronic oscillator frequencies Ω_ν, effective dipole moments $\mu_\nu^{(1)}$, and first (α), third (γ), fifth (δ), and seventh (ζ) off-resonant polarizabilities with the number of modes used for octateraene ($N=8$). Convergence to the full TDHF calculation ($M=16$) is demonstrated. The magnitudes of polarizabilities are normalized at their converged values: $\alpha=3.2\times10^{-23}$ esu, $\gamma=6.6\times10^{-35}$ esu, $\delta=1.4\times10^{-46}$ esu, $\zeta=2.3\times10^{-59}$ esu.

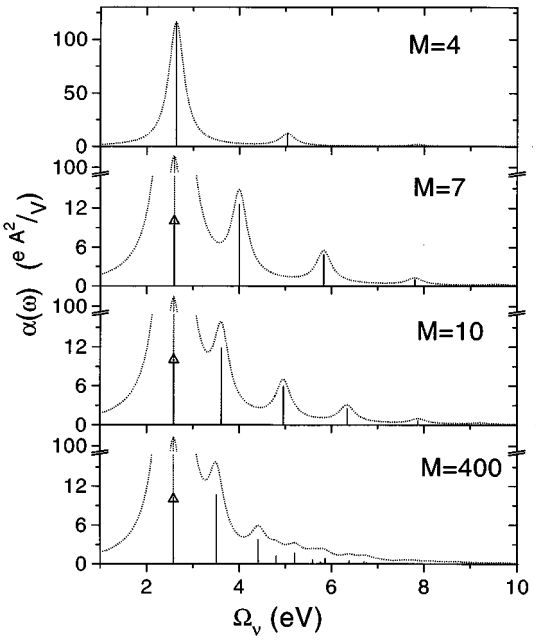

FIG. 2. Convergence of the linear absorption (the imaginary part of α [Eq. (31)]) with the number of modes used for $N=40$ atom oligomer. The linewidth is $\epsilon=0.2$ eV. Note, that the fundamental band at 2.57 eV with strength 109 eÅ^2/V (1.57×10^{-21} esu) remains basically the same in all panels.

lators are natural collective variables which describe in the best way the contribution of all electronic oscillators to the optical response.

The convergence as a function of the number of modes M, $M=1-6$ is shown in Fig. 1 for octatetraene ($N=8$). Only few (3–4) modes contribute significantly to the response, but to calculate them accurately we need to include some additional high frequency modes with very small oscillator strengths. Using six modes we reproduce the frequencies and the first-order effective dipoles $\mu_\nu^{(1)}(\omega=0)$ to 10^{-8} of the values for the full TDHF (16-mode) calculation. The figure also shows that the polarizabilities converge much faster than the frequencies and dipoles of individual modes. The convergence of the linear absorption (the imaginary part of $\chi^{(1)}$ [Eq. (33)] with the number of modes for a $N=40$ atom oligomers is displayed in Fig. 2. Note that the strong band edge transition is reproduced well even at $M=4$. The weaker transitions at higher frequencies require more modes.

Once Ω_ν and μ_ν are calculated and substituted in Eqs. (47), we can then solve these linear equations for the elements of matrices P_ν and Q_ν representing the momenta P_ν and coordinates Q_ν of the desired modes. The calculation is first performed for the linear response $j=1$. The resulting modes are used to calculate the modes for the second-order response ($j=2$) and so forth.

In summary, the DSMA for computing the off-resonant jth-order response involves four steps:

(1) Finding the matrices $S_n^{(j)}(\omega)$ defined as the short-time expansion coefficients of $S^{(j)}(t)=\mathscr{G}_0(t)\,\eta^{(j)}(\omega)$, and the moments $K_n^{(j)}(\omega)$, $n=0,1,...$, [Eqs. (37), (39), (49)];
(2) Solving the nonlinear system of equations (48) for the frequencies Ω_ν and the effective oscillator strengths $f_\nu^{(j)}(\omega)$;
(3) Solving the linear systems of equations (47) for the matrices representing the dominate modes P_ν and Q_ν;
(4) Calculating the jth-order term in the expansion of the density matrix $\xi^{(j)}(\omega)$ [Eq. (46)].

For the third-order response we use $\eta^{(3)}$ and $T^{(3)}$ given by Eqs. (26) and (25). After some algebraic transformations and expanding in the modes, we obtain the eight term expression for γ derived in Ref. 24 which represents the response in terms of quasiparticle scattering.

An alternative form for the jth-order nonlinear response $\chi^{(j)}$ is obtained by rewriting Eq. (27) as

$$\chi^{(j)}=-\frac{1}{\mathscr{E}_0^j}\left[\mathrm{Tr}(\mu\mathscr{G}_0(\omega)\,\eta^{(j)}(\omega))+\mathrm{Tr}(\mu T^{(j)})\right]. \tag{50}$$

We next make use of the fact that for any linear operators $\zeta(\omega)$ and $\vartheta(\omega)$

$$\mathrm{Tr}(\zeta(\omega),\ \mathscr{G}_0(\omega)\,\vartheta(\omega))=\mathrm{Tr}([\mathscr{G}_0(\omega)([\zeta(\omega),\overline{\rho}])\,\vartheta(\omega)],\overline{\rho)} \tag{51}$$

to recast Eq. (50) in the form

$$\chi^{(j)}=-\frac{1}{\mathscr{E}_0^j}\left(\mathrm{Tr}([\xi^{(1)}(\omega),\eta^{(j)}(\omega)],\overline{\rho)}+\mathrm{Tr}(\mu T^{(j)}(\omega))\right). \tag{52}$$

Note that $\eta^{(j)}(\omega)$ and $T^{(j)}(\omega)$ can be expressed in terms of lower order intra- and interband components of the off-resonant density matrix $\delta\rho^{(k)}(\omega)$, $k<j$. Equation (52), therefore, allows us to compute $\chi^{(j)}$ using $\xi^{(1)},\ldots,\xi^{(j-1)}$, avoiding the explicit calculation of $\xi^{(j)}$.

In concluding this section we comment on the connection of the DSMA with the Lanczos algorithm conventionally used for calculating the eigenmodes of Hermitian matrices. The Lanczos algorithm is based on following the short-time evolution determined by a Hermitian operator L, i.e., looking at the quantity $e^{-iLt}\xi$ where ξ is the initial vector, and reducing the space of states to a k-dimensional Krylov subspace[29] generated by $\xi, L\xi,\ldots,L^{k-1}\xi$. We assume that the initial vector ξ can be expanded using a finite number of eigenmodes of L, say, $\xi_0,\ldots,\xi_{k-1}$. The Krylov subspace then coincides with the subspace generated by $\xi_0,\ldots,\xi_{k-1}$, and is invariant with respect to L, $\xi_0,\ldots,\xi_{k-1}$ being linear combination of $\xi, L\xi,\ldots,L^{k-1}\xi$. The problem is now reduced to working in a k-dimensional Krylov subspace, which in many cases is much smaller than the original space. Therefore, the success (i.e., fast convergence) of the Lanczos type schemes depends on the number of eigenmodes with nonzero projection onto the initial vector ξ; the smaller the number, the faster the convergence. This depends crucially on the choice of initial vector. A formally similar procedure is the continued fraction representation of $\int_0^\infty dt e^{i\omega t}\langle\xi|e^{-iLt}|\xi\rangle$,[31] which is also a resummed short-time expansion.

In our case the linearized TDHF operator L is nonhermitian, and our approach is based on an important observation that the operator L is simplectic, i.e., ''hermitian'' with respect to an assymetric ''scalar product'' introduced in Ref. 24 and given by Eq. (29). This ''scalar product'' plays the same role in the DSMA as the usual scalar product in the Lanczos scheme. In the DSMA we apply the Lanczos type scheme in each order of the response, with the effective dipole moment $\mu_\nu^{(j)}$ playing the role of the initial vector ξ. The effective dipole moment is expressed in terms of modes which show up in lower responses and can be computed by applying the short-time propagation for the lower responses. To accomplish this program we need to calculate the eigenvalues as well as the eigenmodes of the Liouville operator. This is done by solving the linear problem whose dimensionality is the number of modes showing up in the expansion of an effective dipole moment. It is at this point that we exploit the dominant mode character of the response, namely that only a few modes show up in this expansion at each order of the response.

V. RESULTS AND DISCUSSION

We have utilized the collective nature of the electronic optical response in conjugated polyenes to construct an efficient algorithm for computing optical nonlinearities using the electronic dominant modes. Since we only need few modes, computational time scales very favorably with system size ($\sim N^2$ compared with $\sim N^6$ for the TDHF[4]). We can, therefore, calculate nonlinear polarizabilities of very large molecules with hundreds of carbon atoms using modest numerical effort. Moreover, the computational time of $\chi^{(m)}$ scales only linearly with m, which allows us to calculate high-order nonlinearities without major difficulty.

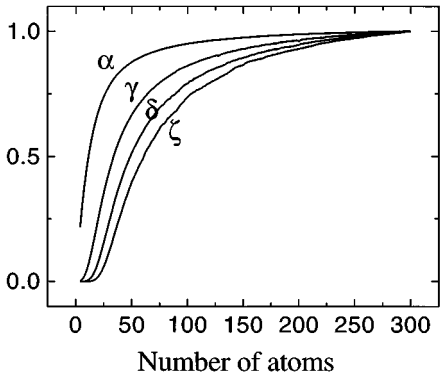

FIG. 3. Scaling of linear α, third-order γ, fifth-order δ, and seventh-order ζ polarizabilities with size. Shown are the magnitudes of polarizability normalized at its saturated value $\chi^{(j)}(N)/N\chi^{(j)}_{\rm sat}$, where $\chi^{(j)}_{\rm sat}=\chi^{(j)}(N)/N$ at $N\to\infty$, $j=1,3,5,7$. The magnitudes of saturated polarizabilities are $\alpha_{\rm sat}=1.7\times10^{-23}$ esu, $\gamma_{\rm sat}=1.1\times10^{-33}$ esu, $\delta_{\rm sat}=1.9\times10^{-43}$ esu, $\zeta_{\rm sat}=5.2\times10^{-53}$ esu.

We have calculated the off-resonant polarizabilities up to seventh order, for polyacetylene oligomers with up to 300 carbon atoms. The variation of the lowest four nonvanishing polarizabilities α, γ, δ, and ζ with the number of carbon atoms N is displayed in the Fig. 3. Since the molecules have an inversion symmetry, antisymmetric (B_u) modes contribute to the odd order responses ($j=1,3,5,7$), whereas the symmetric (A_g) oscillators appear only in the even order responses ($j=2,4,6$). Only 11 B_u and 10 A_g modes (see Fig. 4) were required to obtain a 0.1% accuracy compared with the full ($N^2/4$) modes TDHF calculations (comparisons were made for chains with up to 40 carbon atoms and up to the third-order response, where the full TDHF calculations were

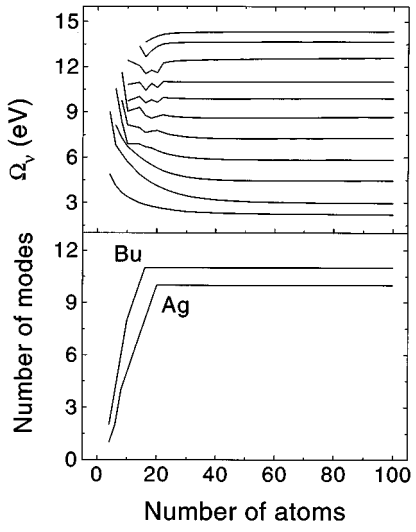

FIG. 4. Upper panel: size dependence of mode frequencies. Lower panel: the number of dominant modes, needed to compute susceptibilities with 0.1% accuracy compared with the full $N^2/4$ modes TDHF calculations.

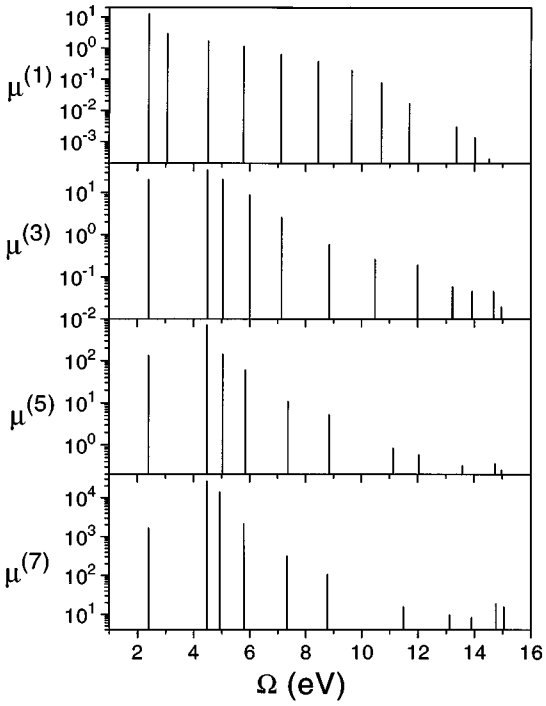

FIG. 5. The effective dipole moments μ_ν vs electronic oscillator frequencies Ω_ν for an $N=100$ polyacetylene chain. Shown are the dominant modes in first, third, fifth, and seventh orders of nonlinearity.

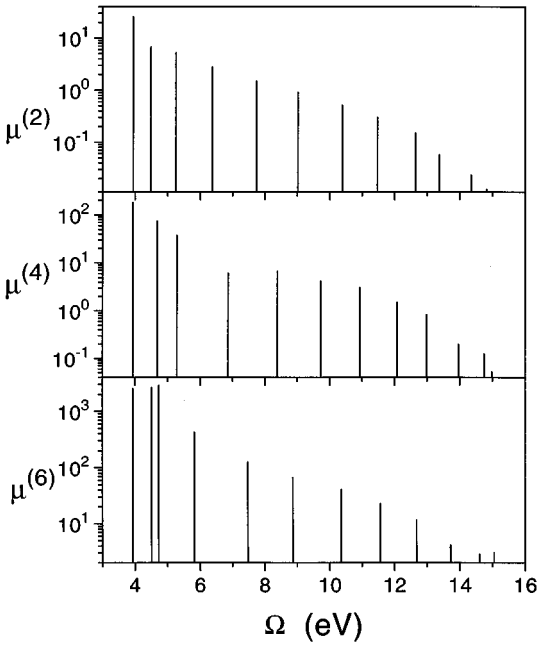

FIG. 6. The effective dipole moments μ_ν vs electronic oscillator frequencies Ω_ν for an $N=100$ polyacetylene chain. Shown are the dominant modes in second, forth, and sixth orders of nonlinearity.

feasible). Comparison of the absolute magnitudes of the calculated polarizabilities with *ab initio* coupled perturbed Hartree–Fock theory[35] show an agreement to within a factor of 1.5 for linear and 2.5 for third-order static polarizabilities. This agreement is very encouraging, in particular given that the present calculations did not employ any geometry optimization.

The effective dipole moments, $\mu_\nu^{(j)}$ [Eq. (46)] of antisymmetric (B_u) and symmetric (A_g) oscillators of a $N=100$ polyacetylene chain are displayed versus mode frequencies Ω_ν in Figs. 5 and 6, respectively. An important observation is that the same modes dominate at all orders. These modes manifest themselves in the response with different effective oscillator strengths at each order. The higher-frequency modes make more significant contributions to the higher order response. The mode size measured by the off-diagonal electronic coherence of its eigenvector grows with its frequency,[4] and, therefore, the coherence size increases for higher-order nonlinearities. This can be seen in Fig. 7 where we display the variation of the scaling exponents $b\equiv d[\ln\chi]/d[\ln N]$, $\chi=\alpha$, γ, δ, and ζ with size. The curves shown in Fig. 5 attain a maximums $b_\gamma=3.5$ at $N_\gamma=8$; $b_\delta=5.7$ at $N_\delta=10$; $b_\zeta=7.9$ at $N_\zeta=12$ (b attains a larger maximum value for calculations with geometry optimization). We note that b reaches a maximum and eventually approaches 1 (saturates). This saturation occurs at longer sizes with increased order of nonlinearity. Measurements of γ in solution as a function of chain length in long chains (up to 240 double bonds) were reported in Ref. 13. The experimental b-curve resembles Fig. 7 with a maximum $b_\gamma=2.5$ for $N_\gamma=60$ double bonds.

We note that the various terms in the effective dipole moment $\eta^{(i)}$ [Eq. (29)] make different contributions to the effective oscillator strengths and to the nonlinear response. This allows us to separate the relative contributions of different processes to the response. As an example, the ratio ($a\equiv\chi_{p-h}^{(j)}/\chi^{(j)}$) of interband contribution to the total polarizability γ, δ, and ζ for oligomers with up to 150 atoms is depicted in Fig. 8. For small chains, the particle–hole contribution is negative in all cases. With increased chain length this contribution changes sign, and for chains longer than the exciton coherence size (~ 30)[4] the ratio saturates to the values $a_\gamma=0.4$; $a_\delta=0.26$; $a_\zeta=0.19$.

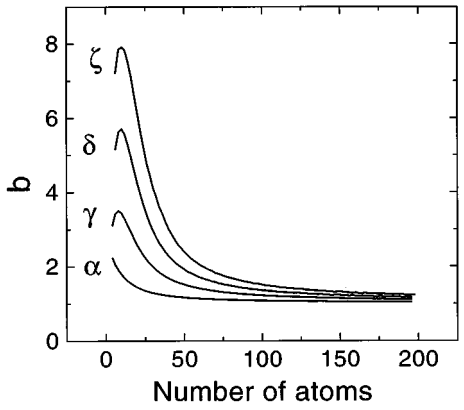

FIG. 7. Variation of the scaling exponents $b\equiv d[\ln\chi]/d[\ln N]$, $\chi=\alpha$, γ, δ, and ζ with size. Note that both the maximum value of b and the size where the maximum is attained increase with the degree of nonlinearity.

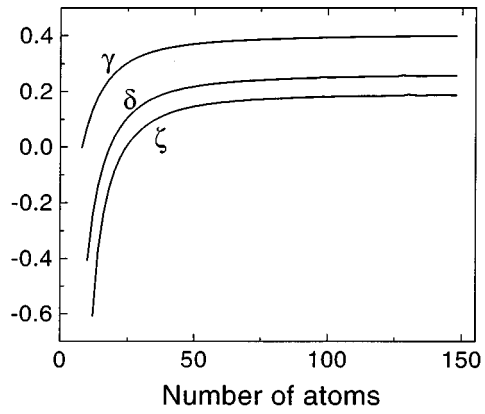

FIG. 8. The ratio of the interband contribution ($a=\chi^{(j)}_{p-h}/\chi^{(j)}$) to γ, δ, and ζ polarizabilities. Note that for small chain lengths the particle–hole contributions to the high order polarizabilities are negative, and the interband contribution decreases with increased degree of nonlinearity. The ratio saturates to the values $a_\gamma=0.4$; $a_\delta=0.26$; $a_\zeta=0.19$.

In addition to its clear numerical advantages, the oscillator representation may be used to develop simple rules of thumb for the scaling of optical polarizabilities with molecular size and chemical bonding. To that end, we have derived in Appendix C analytical expressions for the lowest two nonzero spectral moments of linear absorption $K_0^{(1)}$ and $K_2^{(1)}$. These two moments are then used in Appendix D to construct a single-oscillator analytical approximation for the off-resonant linear polarizability α. In Appendix E we repeat this calculation for the third-order polarizability γ. Based on the results of α and γ, we make the following conjecture for the jth-order off-resonant polarizability

$$\chi^{(j)}=\frac{j(ea)^{j+1}}{2(4\beta'\Delta)^j}\,k_j\,\frac{N^{j+1}}{[N+L(\Delta)]^j}. \tag{53}$$

Here e is the electron charge, a is the unit cell size along the backbone, Δ is the average bond-length alternation parameter (i.e., the difference between nearest-neighbor bond lengths), β' is the electron–phonon coupling constant,[4] and L is the effective coherence size (see Appendix C). This approximation, which lumps the contribution of all electronic oscillators into a single effective oscillator, reproduces the main features of the scaling exponent b, and compares well with full TDHF calculations.[36]

In concluding this article we discuss some possible future extensions of DMSA. First, the algorithm is not limited to the semiempirical PPP model and it can be combined with *ab initio* electronic structure calculations using different basis sets, and applied to more complicated molecules as well as to semiconductor nanostructures.[37–39]

In this paper we only reported numerical calculations for the off-resonant polarizabilities; however, the extension to the resonant regime is straightforward. One can use the procedure described in Appendix D of Ref. 4 to compute the frequency-dependent effective dipole moments $\mu^{(j)}(\omega)$, and the intraband components $T^{(j)}(\omega)$ of the density matrix $\delta\rho^{(j)}(\omega)$, or calculate the dominant modes first using the DSMA for off-resonant response and then obtain the anharmonicity constants introduced in Ref. 24 which contain all relevant information about the resonant response (both time and frequency domain). The accuracy of the DSMA depends heavily on the accuracy of the ground state density matrix $\overline{\rho}$, because we apply a commutator with $\overline{\rho}$ [or with $V(\overline{\rho})$] $8k$ times for calculating $K_k^{(j)}$. This leads to increased errors in the higher moments, especially in long chains and for high-order responses. Using double precision we obtained very accurate results for the optical response and the most dominant (1–2) modes contributing to this response. Resonant calculations performed with a frequency-dependent dipole moment should allow us to focus on the desired spectral range and obtain a good accuracy. Another way to accomplish that is to use a crude approximation for ξ_ν obtained in an off-resonant calculations as an effective dipole moment. This dipole moment will be coupled strongly with the desired single mode, which can then be extracted accurately using the DSMA.

Since the same modes are dominant at low and high orders, we anticipate that this set of modes may be used to compute the response to all orders. In Ref. 24 the restricted TDHF equations were written in the oscillator representation. By combining these equations with the present dominant modes picture, one can find the nonlinear response by solving a closed system of equations with only small number of variables. This means that the equations of motion of Ref. 24 in the mode representation, derived using the modes which dominate the response up to third order, can be applied to calculate the response to a strong external field.

Another interesting future direction is to extend the DSMA beyond the TDHF scheme, to treat electron correlations more rigorously. This extension is based on the observation[24] that the TDHF approximation is the classical analog of the original model. The dominant picture of the response in all orders implies that evolution of the classical system occurs in the reduced phase space. Quantizing the TDHF equations written in the dominant mode representation (i.e., quantizing the reduced classical system) using the procedure of geometrical quantization,[40] one can obtain an effective multilevel system with space of states dimensionality that depends on the number of dominant TDHF modes rather then the molecule size. This effective quantum system should maintain all the important features of the original one, and should allow a nonperturbative calculation of strong electron correlations, by treating explicitly the quantum evolution of relevant (dominant) variables, which is achieved by working in the effective multilevel quantum space.

ACKNOWLEDGMENTS

The support of the U.S. Air Force Office of Scientific Research and the National Science Foundation is gratefully acknowledged.

APPENDIX A: THE INTRABAND COMPONENTS $T(\xi)$ OF THE DENSITY MATRIX [EQS. (8)–(10)]

The single-electron reduced density matrix in the TDHF approximation satisfies the condition $\rho^2(t)=\rho(t)$ at all times.[4,24,25] Using Eq. (7) this results in

$$(\overline{\rho}+\xi(t)+T(\xi(t)))^2=\overline{\rho}+\xi(t)+T(\xi(t)). \tag{A1}$$

The intraband part of this matrix equation is

$$(T(\xi))^2+(2\overline{\rho}-I)T(\xi)+\xi^2=0. \tag{A2}$$

The solution of this equation, with the condition $T(\xi=0)=0$ yields Eq. (8).

To obtain Eq. (10) we first note that the algebra $\mathscr{A}$ of reduced density matrices can be decomposed (as a vector space) into a direct sum of intraband ($\mathscr{A}_0$) and interband ($\mathscr{A}_1$) density matrices

$$\mathscr{A}=\mathscr{A}_0\oplus\mathscr{A}_1, \tag{A3}$$

with the following properties of the commutators:

$$[\xi,\eta]\in\mathscr{A}_0, \quad \text{for } \xi,\eta\in\mathscr{A}_0, \quad \text{or} \quad \xi,\eta\in\mathscr{A}_1, \tag{A4}$$

and

$$[\xi,\eta]\in\mathscr{A}_1, \quad \text{for } \xi\in\mathscr{A}_0 \text{ and } \eta\in\mathscr{A}_1. \tag{A5}$$

Any density matrix ρ satisfying the constraint $\rho^2=\rho$, i.e., $\rho\in\mathscr{M}$, where $\mathscr{M}$ is the Grassman manifold[24] becomes

$$\rho=g\overline{\rho}g^{-1}, \tag{A6}$$

where g is a unitary matrix. Since any g in a vicinity of a unit matrix can be represented in a form $g=\exp(\eta)$ with $\eta\in\mathscr{A}$ Eq. (A6) can be represented in a form

$$\rho=\exp(\eta)\overline{\rho}\exp(-\eta), \tag{A7}$$

or adopting the language of superoperators (i.e., operators acting in Liouville space)

$$\rho=\exp(\tilde{\eta})\overline{\rho}, \tag{A8}$$

where for any $\eta\in\mathscr{A}$ the superoperator $\tilde{\eta}$ is defined by

$$\tilde{\eta}\xi\equiv[\eta,\xi] \quad \text{for } \xi\in\mathscr{A}. \tag{A9}$$

Expanding the exponent in Eq. (A8) in the superoperator $\tilde{\eta}$ and making use of Eq. (A9) we obtain

$$\rho=\overline{\rho}+[\eta,\overline{\rho}]+\frac{1}{2}[\eta,[\eta,\overline{\rho}]]+\frac{1}{3!}[\eta,[\eta,[\eta,\overline{\rho}]]]+\cdots. \tag{A10}$$

Comparing Eqs. (7) with (A10) results in the linear approximations in η

$$\xi\cong[\eta,\overline{\rho}]. \tag{A11}$$

Since $[\overline{\rho},[\overline{\rho},\xi]]=\xi$ for any $\xi\in\mathscr{A}_1$,[24] Eq. (A10) constitutes a one-to-one mapping between $\mathscr{A}_1$ and the tangent space to $\mathscr{M}$ at the point $\overline{\rho}$. This implies that we can always choose $\eta\in\mathscr{A}_1$ in the expansion of Eq. (A10). For this choice, the even-order terms in the expansion belong to $\mathscr{A}_0$, the odd to $\mathscr{A}_1$ [this follows from Eqs. (A4) and (A5) and the fact that $\overline{\rho}\in\mathscr{A}_0$]. Combining Eqs. (A10) and (A4) then yields

$$\xi=[\eta,\overline{\rho}]+\frac{1}{3!}[\eta,[\eta,[\eta,\overline{\rho}]]]+\cdots. \tag{A12}$$

$$T=\frac{1}{2}[\eta,[\eta,\overline{\rho}]]+\frac{1}{4!}[\eta,[\eta,[\eta,\overline{\rho}]]]+\cdots. \tag{A13}$$

To derive Eq. (10) we solve Eq. (A12) to express η in terms of ξ, and then substitute η into Eq. (A13). Equation (A12) may be solved iteratively leading to an expansion of η in powers of ξ which can be calculated to any order in ξ and has a form

$$\eta=[\xi,\overline{\rho}]-\frac{1}{3!}[\kappa,\overline{\rho}]+\cdots \tag{A14}$$

with

$$\kappa\equiv[[\xi,\rho],[[\xi,\overline{\rho}],\xi]]. \tag{A15}$$

Substituting Eq. (A14) into Eq. (A13) finally yields the expansion of Eq. (10).

APPENDIX B: SOLUTION OF EQS. (48)

The system of nonlinear equations (48) may be solved as follows. Let us consider the following system of $2n$ equations with respect to n ''nonlinear'' frequency Ω_n and n ''linear'' oscillator strength f_n variables

$$\begin{aligned}
&K_0=f_1+f_2+f_3+\cdots+f_n,\\
&K_1=f_1\Omega_1^2+f_2\Omega_2^2+\cdots+f_n\Omega_n^2,\\
&K_2=f_1\Omega_1^4+f_2\Omega_2^4+\cdots+f_n\Omega_n^4,\\
&\qquad\cdots\\
&K_{n-1}=f_1\Omega_1^{2(n-1)}+f_2\Omega_2^{2(n-1)}+\cdots+f_n\Omega_n^{2(n-1)},\\
&K_n=f_1\Omega_1^{2n}+f_2\Omega_2^{2n}+\cdots+f_n\Omega_n^{2n},\\
&\qquad\cdots\\
&K_{2n-1}=f_1\Omega_1^{2(2n-1)}+f_2\Omega_2^{2(2n-1)}+\cdots+f_n\Omega_n^{2(2n-1)}.
\end{aligned} \tag{B1}$$

The frequency variables $\Omega^2=x$ are the roots of the polynomial

$$x^n-a_1x^{n-1}-a_2x^{n-2}-\cdots-a_{n-1}x-a_n, \tag{B2}$$

where the coefficients a_i, $i=1,\cdots,n$ are the solution of system of n linear equations

$$\begin{aligned}
&K_n=K_{n-1}a_n+K_{n-2}a_{n-1}+K_{n-3}a_{n-2}+\cdots+K_1a_2\\
&\qquad+K_0a_1,\\
&K_{n+1}=K_na_n+K_{n-1}a_{n-1}+K_{n-2}a_{n-2}+\cdots+K_2a_2\\
&\qquad+K_1a_1,\\
&K_{n+2}=K_{n+1}a_n+K_na_{n-1}+K_{n-1}a_{n-2}+\cdots+K_3a_2\\
&\qquad+K_2a_1,\\
&\qquad\cdots\\
&K_{2n-1}=K_{2n-2}a_n+K_{2n-3}a_{n-1}+K_{2n-4}a_{n-2}+\cdots\\
&\qquad+K_na_2+K_{n-1}a_1.
\end{aligned} \tag{B3}$$

To rationalize Eqs. (B2) and (B3) we note that Viet's theorem[41] establishes the relationship between the polynomial roots and coefficients

$$\begin{aligned} a_1 &= x_1 + x_2 + \cdots + x_n, \\ a_2 &= -\sum_{i_1<i_2} x_{i_1} x_{i_2}, \\ &\cdots \\ a_k &= (-1)^{(k+1)} \sum_{i_1<i_2<\cdots<i_k} x_{i_1} x_{i_2} \cdots x_{i_k}, \\ &\cdots \\ a_n &= (-1)^{(n+1)} x_1 x_2 \cdots x_n . \end{aligned} \tag{B4}$$

To verify Eqs. (B3) we simply substitute Eqs. (B4) in the expression for K_n (B3)

$$\begin{aligned} K_n &= \left(\sum_i f_i x_i^{n-1} \right) \left(\sum_j x_j \right) - \left(\sum_i f_i x_i^{n-2} \right) \\ &\quad \times \left(\sum_{j_1<j_2} x_{j_1} x_{j_2} \right) + \cdots \\ &= \sum_i f_i x_i^n + \sum_{i \neq j} f_i x_i^{n-1} x_j - \left(\sum_i f_i x_i^{n-2} \right) \\ &\quad \times \left(\sum_{j_1<j_2} x_{j_1} x_{j_2} \right) + \cdots \\ &= K_n - \sum_{i \neq (j_1<j_2)} f_i x_i^{n-2} x_{j_1} x_{j_2} + \left(\sum_i f_i x_i^{n-3} \right) \\ &\quad \times \left(\sum_{j_1<j_2<j_3} x_{j_1} x_{j_2} x_{j_3} \right) - \cdots \\ &= \cdots = K_n + (-1)^n \sum_{i \neq (j_1<\cdots<j_{n-1})} f_i x_i x_{j_1} \cdots x_{j_{n-1}} \\ &\quad + (-1)^{n+1} \sum_i f_i x_1 x_2 \cdots x_n = K_n . \end{aligned} \tag{B5}$$

Thus, all terms (except K_n) in the right-hand side of Eq. (B5) vanish, leaving the identity $K_n \equiv K_n$.

Equations (B3) is known as the Toeplitz linear system. The inversion of the Toeplitz matrices is straightforward[42] and poses no numerical difficulties.

Once the frequencies are found, the oscillator strengths can be computed by solving the linear system of the first n equations of (B1) for the variables f_n. Thus, the solution of the nonlinear system (B1) is obtained in three steps: two sets of linear equations, and finding the zeros of a polynomial with real coefficients (the only nonlinear task).

Since $f_1 \ll f_2 \ll f_3 \ll \cdots \ll f_n$, and $\Omega_1^n \gg \Omega_2^n \gg \cdots \gg \Omega_n^n$, the lower frequency terms are dominant in the first equations of system (B1) and the higher frequency terms dominate the higher ones. This allows us to increase the accuracy of the low frequencies by adding new high frequency modes (and the necessary higher moments).

APPENDIX C: EVALUATION OF THE LOWEST TWO MOMENTS OF LINEAR ABSORPTION

In Appendices C–E we will introduce renormalized spectral moments which are independent on the applied static field

$$f^{(2k)} \equiv -\frac{1}{\mathscr{E}_0} K_k^{(1)}, \tag{C1}$$

and the oscillator strengths

$$f_\nu \equiv -\frac{1}{\mathscr{E}_0} f_\nu^{(1)} . \tag{C2}$$

We can then recast a family of sum rules for the linear response [Eq. (48)] as

$$\begin{aligned} f^{(n)} &= \sum_{\nu=1}^{M} (\Omega_\nu)^n f_\nu, \quad n = 0,2,4,\ldots, \\ f^{(n)} &\equiv 0, \quad n = 1,3,5,\ldots . \end{aligned} \tag{C3}$$

To invoke the single-oscillator approximation ($M=1$) for the off-resonant response, we need to express the lowest two spectral moments for the linear response $f^{(0)}$ and $f^{(2)}$ in terms of the Hamiltonian parameters and the ground state reduced density matrix $\overline{\rho_{mn}}$.

In the Hamiltonian [Eq. (1)] we recast a nearest-neighbor hopping Su–Schrieffer–Heeger (SSH) model and electron–electron Coulomb interactions (Ohno formula) as

$$t_{n,n\pm1} = \beta + (-1)^n \beta' \Delta, \quad V_{nm} = U v_{n-m}, \tag{C4}$$

where Δ is the bond-length alternation parameter and v_{n-m} is a dimensionless function (with $v_0 = 1$). We assume that the bond-length alternation only enters through the hopping matrix given by Eq. (C4) and neglect its effect on the Coulomb interaction. For simplicity we shall neglect, when possible, the alternation in the transfer parameter making use of $\Delta \ll a$. This is justified when the electron–phonon contribution to the gap is much smaller than the Coulomb contribution.[34]

Applying the results of Ref. 28 to the system described by Eqs. (C4) and (2) we obtain

$$f^{(0)} = A\beta; \quad f^{(2)} = B_0 \beta^3 + B_1 \beta^2 U, \tag{C5}$$

with

$$\begin{aligned} A &\equiv 4e^2a^2 \sum_n \overline{\rho_{n,n+1}}, \quad B_0 \equiv 8e^2a^2 \overline{\rho_{n_L,n_L+1}}, \\ B_1 &\equiv 2e^2a^2 \left\{ 2 \sum_{m \neq n} v_{m-n} \delta\overline{\rho_n} \delta\overline{\rho_m} + \sum_n (\delta\overline{\rho})^2 \right. \\ &\quad \left. - \sum_{m \neq n} v_{m-n} (\delta\overline{\rho_{mn}})^2 - \sum_{mn} \delta\overline{\rho_{mn}} \delta\eta_{mn} \right\}. \end{aligned} \tag{C6}$$

Here n_L, n_R denote the chain edges, and we have introduced the following definitions

$$\begin{aligned} \eta_{mn} &\equiv -v_{m-n} \overline{\rho_{mn}} (1 - \delta_{mn}) \\ &\quad + \left(2 \sum_{k \neq n} v_{n-k} \overline{\rho_{kk}} + \overline{\rho_{nn}} \right) \delta_{mn}, \end{aligned} \tag{C7}$$

and for an arbitrary matrix ξ_{mn} we define

$$\delta\xi_n \equiv \xi_{n+1,n} - \xi_{n,n-1};$$

$$\delta\xi_{mn} \equiv (\xi_{m-1,n} - \xi_{m,n+1}) - (\xi_{m+1,n} - \xi_{m,n-1}). \tag{C8}$$

To analyze the size scaling of the moments, we note that for large sizes we have $f^{(n)} \sim N$ for all n. Numerical results for $\overline{\rho_{mn}}$ show that boundary effects on $\overline{\rho_{mn}}$ are short range,[4] and only affect it when the distance of m and n from an edge is one or two atoms. This suggests that boundary effects on the sum rules are also short range, and for $N > 10$ say, $f^{(n)}$ can be written in a form

$$f^{(n)} = N f_0^{(n)} + f_1^{(n)}, \tag{C9}$$

where $f_0^{(n)}$ is related to the $N \to \infty$ behavior, and $f_1^{(n)}$ represent edge effects in the sum rules. Careful examination of the sum rules shows that the largest corrections to Eq. (C9) are $\sim N^{-1}$ and $\sim N^{-1} \ln N$, which can be neglected for $N \geqslant 10$. Expressions for $f_0^{(n)}$ and $f_1^{(n)}$ can be obtained by inspecting the behavior of $f^{(n)}$ for large N: $f_0^{(n)}$ are expressed in terms of the saturated components of $\overline{\rho_{mn}}$, i.e., the values of $\overline{\rho_{mn}}$ for large N when m and n are far from the edges, while $f_1^{(n)}$ involves the values of $\overline{\rho_{mn}}$ near the edges (note that $\overline{\rho_{mn}}$ is strongly localized in $m-n$). Making use of Eqs. (C5) and (C6), we obtain from the first moment ($n=0$)

$$f_j^{(0)} = A_j \beta; \quad j = 0,1, \tag{C10}$$

with

$$\begin{aligned} A_0 &\equiv 2e^2a^2(\tilde{\rho}_{n,n+1} + \tilde{\rho}_{n+1,n+2}), \\ A_1 &\equiv 4e^2a^2 \sum_n (\overline{\rho}^{(1)}_{n,n+1} - \tilde{\rho}_{n,n+1}). \end{aligned} \tag{C11}$$

Here $\tilde{\rho}_{mn}$ are the saturated values of the ground state density matrix in a large chain ($N \to \infty$) when m and n are far from the edges n_L and n_R. Therefore, $\tilde{\rho}_{mn}$ can be formally treated as the ground state reduced density matrix of an infinite chain ($-\infty < m, n < +\infty$). $\tilde{\rho}_{mn} = \tilde{\rho}_{n+2k,m+2k}$. $\overline{\tilde{\rho}}^{(1)}_{mn}$ denote the saturated values of $\overline{\rho_{mn}}$ in a large chain ($N \to \infty$) when m and n are far from one of the edges, namely n_R. We can put $n_L = 0$ and for $n_R = N-1 \to \infty$ formally treat $\overline{\rho}^{(1)}_{mn}$ (with $m,n \geqslant 0$) as the ground state density matrix in a semi-infinite chain. Note that neither $\tilde{\rho}_{mn}$ nor $\overline{\rho}^{(1)}_{mn}$ depend on N since they represent the saturated values of ρ_{mn}. $\overline{\rho}^{(1)}_{mn}$, however, carries information about the near-edge values of $\overline{\rho_{mn}}$ when N is large enough and it is not affected by the other edge. For $m,n \gg 1$ we have $\overline{\rho}^{(1)}_{mn} \approx \tilde{\rho}_{mn}$.

For the third moment ($n=2$) we obtain

$$f_j^{(2)} = B_{j0}\beta^3 + B_{j1}\beta^2 U, \tag{C12}$$

with

$$B_{00} = 0,$$

$$B_{10} = 8e^2a^2 \overline{\rho}^{(1)}_{0,1},$$

$$\begin{aligned} B_{01} \equiv e^2a^2 \Big\{ & 2\sum_{m \neq n} v_m (\delta\tilde{\rho}_0 \delta\tilde{\rho}_m + \delta\tilde{\rho}_1 \delta\tilde{\rho}_{m+1}) + (\delta\tilde{\rho}_0)^2 \\ & + (\delta\tilde{\rho}_1)^2 - \sum_{m \neq 0} v_m [(\delta\tilde{\rho}_{m0})^2 + (\delta\tilde{\rho}^{\,2}_{m+1,1})] \\ & - \sum_m (\delta\tilde{\rho}_{m0} \delta\tilde{\eta}_{m0} + \delta\tilde{\rho}_{m+1,1} \delta\tilde{\eta}_{m+1,1}) \Big\}, \end{aligned} \tag{C13}$$

$$B_{11} = 4e^2a^2 \sum_n b_n,$$

$$\begin{aligned} b_n \equiv{}& 2\delta\overline{\rho}^{(1)}_n \sum_{m \neq n} v_{m-n} \delta\overline{\rho}^{(1)}_m + (\delta\overline{\rho}^{(1)}_n)^2 \\ & - \sum_{m \neq n} v_{m-n} (\delta\overline{\rho}^{(1)}_{mn})^2 - \sum_m \delta\overline{\rho}^{(1)}_{mn} \delta\eta^{(1)}_{mn} \\ & - \frac{1}{e^2a^2} B_{01}. \end{aligned}$$

In Eq. (C13) we have formally extended $\overline{\rho}^{(1)}_{mn}$ to arbitrary m and n setting $\overline{\rho}^{(1)}_{mn} = 0$ when $m < 0$, or $n < 0$.

On the other hand, making use of the stationary HF equation for an infinite chain, we obtain the following relation between the parameters $\beta_j \equiv \beta - (-1)^j \beta' \Delta$, $j = 0$, 1, and U

$$\beta_j = C_j^{-1} U, \quad j = 0,1. \tag{C14}$$

The expansion of Eq. (C12) can be obtained from the sum rules for a chain. The easiest way to obtain Eq. (C14) and calculate C_j is to apply the stationary HF equation (which is a matrix equation) to the n, $n+1$ component. This yields

$$\begin{aligned} C_j^{-1} = [\tilde{\rho}_{j+2,j} - \tilde{\rho}_{j+1,j-1}]^{-1} \sum_m & (\tilde{\rho}_{2m+j+1,j+1} - \tilde{\rho}_{2m+j,j}) \\ & \times (\tilde{\rho}_{2m+j+1,j+2} v_{2m-1} - \tilde{\rho}_{2m+j+1,j-1} v_{2m}). \end{aligned} \tag{C15}$$

The most important fact is that the coefficients A, B, and C do not explicitly depend on N or on the parameters of the Hamiltonian β, β', U; they are expressed in terms of the bond-length alternation and the ground state density matrix $\overline{\rho_{mn}}$ in a long chain, which can be obtained in practice by performing a single calculation for a large chain (say $N \sim 50$).

Combining Eqs. (C9), (C12), and (C14) and setting $C_0 \approx C_1 \equiv C$, we obtain

$$f^{(0)} = A_0 \beta (N + L_0), \tag{C16}$$

$$f^{(2)} = (B_{00} + B_{01} C) \beta^3 (N + L_1) \tag{C17}$$

with

$$L_0 \equiv \frac{A_1}{A_0}, \quad L_1 \equiv \frac{B_{10} + B_{11} C}{B_{00} + B_{01} C}. \tag{C18}$$

Equations (C5)–(C18) express the linear spectral moments of density matrix in terms of the parameters of the Hamiltonian and $\overline{\rho_{mn}}$. This constitutes an important structure polarizability relationship, which predicts the magnitude of the optical response using detailed information regarding the chemical structure and bonding. These results will be used in Appendix D.

APPENDIX D: SINGLE-OSCILLATOR APPROXIMATION FOR THE LINEAR RESPONSE

By employing the identities (43) and (C2) to Eq. (33), we can write the off-resonant linear polarizability as

$$\alpha(\omega=0)=\sum_{\nu=1}^{M}\frac{f_\nu}{\Omega_\nu^2}. \tag{D1}$$

We now consider the lowest approximation ($M=1$) of the hierarchy Eqs. (D1) and (C3), where we retain only a single oscillator. This approximation is exact if the oscillator strength is concentrated in one oscillator. However, its range of validity goes far beyond this case since it approximates the contributions of all oscillators by a single effective one. Making use of Eq. (C3) for $k=0$, 1 and Eq. (D1) we obtain for the off-resonant polarizability $\alpha\equiv\alpha(\omega=0)$ and the optical gap Ω

$$\alpha=\frac{[f^{(0)}]^2}{f^{(2)}},\quad \Omega=\left[\frac{f^{(2)}}{f^{(0)}}\right]^{1/2}. \tag{D2}$$

Substituting Eqs. (C16) and (C17) into Eq. (D2) yields

$$\alpha(N)=\frac{\kappa}{\beta}\frac{(N+L_0)^2}{N+L_1}, \tag{D3}$$

$$\Omega(N)=\left(\frac{N+L_1}{N+L_0}\right)^{1/2}\tilde{\Omega}, \tag{D4}$$

where the parameters κ and $\tilde{\Omega}$, which characterize the values of the linear response and the optical gap in long molecules, have the form

$$\kappa=\frac{A_0^2}{B_{00}+B_{01}C},\quad \tilde{\Omega}=\left(\frac{B_{00}+B_{01}C}{A_0}\right)^{1/2}\beta. \tag{D5}$$

Equations (D3) and (D4) together with Eqs. (C18) and (D5) express the off-resonant linear polarizability $\alpha(N)$ in terms of ground state properties of large molecules.

At this point we estimate the coherence sizes L_0 and L_1 and connect L_1 with the magnitude of bond alternation. The coherence size L_0 is related to $f^{(0)}$, and since edge effects of $\overline{\rho}$ are short range, $L_0\sim 1$. The situation is quite different for the coherence size L_1 related to $f^{(2)}$. It follows from Eqs. (C6)–(C8), that in a translationally invariant system $f^{(2)}=0$. This also follows immediately from the corresponding sum rule presented in Ref. 28, which is written in terms of commutators, since translationally invariant matrices commute. Two factors may break the translational symmetry in finite chains: spontaneous symmetry breaking, which leads to the alternation in parameters, and boundary (edge) effects. The first mechanism (which exists even in an infinite chain) leads to a $\sim N$ contribution to $f^{(2)}$ which decreases with decreased bond alternation. The second mechanism leads to a finite (i.e., $\sim N^0$) contribution to $f^{(2)}$ which is independent of the alternation parameter. Equations (C13) show that $f_0^{(2)}$ has an extra small factor compared to $f_1^{(2)}$ related to the bond-length alternation parameter in an infinite chain,[4] and for weak alternations we have $L_1\gg L_0$, which means that we can neglect L_0 while retaining L_1 in Eqs. (D3) and (D4). On the other hand the fact that $f_0^{(2)}$ has small a factor means that the parameter $B_{00}+B_{01}C$ in Eq. (C17) is small provided effects of alternation are weak. Numerical calculations of Ref. 36 show it scales as $B_{00}+B_{01}C\sim\beta'\Delta$ with bond-length alternation. We can then recast the parameter κ in the form

$$\kappa=\frac{(ea)^2\beta}{8\beta'\Delta}k_1 \tag{D6}$$

with k_1 weakly dependent on Δ. Combining Eqs. (D3), (D4), and (D6) and making use of the above arguments we finally obtain:

$$\Omega(N)=\left(\frac{N+L_1}{N}\right)^{1/2}\tilde{\Omega}, \tag{D7}$$

$$\alpha(N)=\frac{(ea)^2}{8\beta'\Delta}k_1\frac{N^2}{N+L_1}, \tag{D8}$$

with the following scaling of $\tilde{\Omega}$ and L_1 with Δ: $\tilde{\Omega}^2\sim\Delta$, $L_1\sim\Delta^{-1}$. Numerical calculations of Ref. 36 show $k_1\sim 1$. Equations (D7) and (D8) imply that for large N, $f^{(0)}(N)\sim N$, $\alpha(N)\sim N$, and $\Omega(N)$ is independent of N whereas for small N, $f(N)\sim N$, $\alpha(N)\sim N^2$ and $\Omega(N)\sim N^{-1/2}$.

This establishes a direct relation between the scaling properties of the off-resonant polarizability to chemical properties of conjugated molecules. L_1 is thus the coherence size which determines the crossover of the short and long chain behaviors of $\alpha(N)$ and $\Omega(N)$. The simple relations of Eqs. (D7) and (D8) are in a good agreement with full TDHF calculations.[36]

APPENDIX E: SIZE SCALING OF THE THIRD-ORDER RESPONSE

The calculation of the third-order nonlinear polarizability γ is much more tedious than α, even when only a few modes dominate. The TDHF expression for γ has eight contributions,[24] and each dominant oscillator ν contains two variables ($\hat{\xi}_\nu$ and $\hat{\xi}_\nu^+$ or $\hat{P}_\nu$ and $\hat{Q}_\nu$). The number of coefficients becomes very large, and we need a large number of sum rules to determine them, which greatly complicates the picture. To derive a simple yet qualitatively correct expression, we make some additional assumptions. Numerical TDHF calculations of the optical response show that processes which do not conserve the number of electron–hole pairs can be treated perturbatively. Neglecting these processes leads to the following relevant level scheme for the third-order response: the ground (vacuum) state with no electron–hole pairs (excitons), one-exciton states with B_u symmetry, and two-exciton states with A_g symmetry, which are made out of two B_u excitons. Processes which do not conserve the number of excitons mix the two-exciton states consisting of two B_u excitons and one-exciton A_g states.[43] There are two kinds of A_g states contributing to γ: (i) $2B_u$ states with a small component of $1A_g$, and (ii) $1A_g$ states with a small component of $2B_u$ states. The latter lead to sharp two-photon resonances in γ and show up in the TDHF approximation as resonances related to A_g oscillators. The former states to a certain extend are taken into account by the TDHF approximation, which fails near two-photon reso-

nances on these states. This is, however, not important for the off-resonant response. The contribution of states (ii) is essential for the resonant properties of γ (e.g., two-photon absorption); however, their contribution to the off-resonant response is small provided the processes which do not conserve the number of excitons are weak. Adopting TDHF terminology, the contributions of (i) and (ii) states are related to the terms in the expressions of Ref. 24 which do not and do contain respectively A_g oscillators (which further lead to sharp two-photon resonances). Assuming that processes which do not conserve the number of excitons are weak, we will take into account only those terms which do not contain the A_g oscillators.[24] This still leaves us with a large number of terms related to summations over indices denoting the momentum and coordinate variables of each oscillator. This number can be considerably reduced when the terms induced by processes which do not conserve the number of excitons are neglected (formally this means that the eigenmodes $\hat{\xi}_\alpha$ and $\hat{\xi}_\alpha^+$ contain the particle–hole and hole–particle components of the density matrix respectively). If in addition we assume a single dominant B_u oscillator, we obtain the considerably simplified form of the third-order response function:

$$\gamma(-\omega_s;\omega_1,\omega_2,\omega_3)=\frac{1}{6}\sum_{\text{perm}}\left\{I_1\,\frac{1}{\omega_1-\Omega+i\eta}\,\frac{1}{\omega_2+\Omega+i\eta}\left[\frac{1}{\omega_1+\omega_2+\omega_3-\Omega+i\eta}-\frac{1}{\omega_1+\omega_2+\omega_3+\Omega+i\eta}\right]\right.$$
$$+I_2\,\frac{1}{\omega_1-\Omega+i\eta}\,\frac{1}{\omega_2+\Omega+i\eta}\left[\frac{1}{\omega_3-\Omega+i\eta}\,\frac{1}{\omega_1+\omega_2+\omega_3-\Omega+i\eta}\right.$$
$$\left.\left.+\frac{1}{\omega_3+\Omega+i\eta}\,\frac{1}{\omega_1+\omega_2+\omega_3+\Omega+i\eta}\right]\right\}+\text{c.}'\text{c.}', \tag{E1}$$

where Σ_{perm} stands for a sum of six permutations of the frequencies ω_1, ω_2, and ω_3; c.′c.′ denotes complex conjugation and changing the signs of all frequencies ω_1, ω_2, and ω_3.

γ is now expressed in terms of two parameters I_1 and I_2 which may be determined by applying two sum rules. Switching Eq. (E1) to the time domain and substituting it into the sum rules of Ref. 28 we obtain the following system of equations for I_1 and I_2.

$$\Omega I_1-I_2=\frac{3e^2a^2}{2}\,f^{(0)},$$
$$\Omega^2 I_2=\frac{3e^2a^2}{4}\,f^{(2)}. \tag{E2}$$

Solving Eqs. (E2), substituting I_1 and I_2 into Eq. (E1), and further setting $\omega_1=\omega_2=\omega_3=0$ we obtain for the off-resonant hyperpolarizability γ:

$$\gamma=\frac{3e^2a^2f^{(0)}}{\Omega^4}. \tag{E3}$$

Finally, making use of Eqs. (C16), (D7), and the fact that $\tilde{\Omega}^2\sim\Delta$ we express the off-resonant third-order hyperpolarizability γ in terms of Δ and the ground state reduced density matrix in a large molecule

$$\gamma=\frac{3e^4a^4}{2(4\beta'\Delta)^{m-1}}\,k_3\,\frac{N^m}{(N+L_1)^{m-1}}, \tag{E4}$$

with $m=3$, and the dimensionless coefficient k_3 depends on the ground state single-electron density matrix.

One can apply similar arguments individually to each of the eight contributions to the third order polarizability.[24] This will involve two generalizations of the procedure presented above. First, we need to include the higher order moments of the nonlinear response. Second, instead of using the dipole operator μ in the sum rules for the third-order response given in Ref. 28 we will consider its interband and intraband components given by $[\overline{\rho},[\overline{\rho},\mu]]$ and $\mu-[\overline{\rho},[\overline{\rho},\mu]]$, respectively. New sum rules apply not to the third-order polariability γ but rather for each of eight contributions to γ itself presented in Ref. 24. The procedure is lengthy and rather tedious and will not be given here. The result is that the N and Δ dependence of each contribution is given by Eq. (E4) with b assuming values $m=3,4,5$ for different contributions. We have fitted the results for $\gamma(N)$ obtained by the TDHF calculations using the full DSMA described with the expression of Eq. (E4) for different values of Δ using k_3 and b as fitting parameters. We found that $m=4$ applies over a broad range of variation of Δ, k_3 is order 1 and has a weak dependence on Δ. Numerical results are presented in Ref. 36.

[1] J. F. Heflin, K. Y. Wong, Q. Zamani-Khamini, and A. F. Garito, Phys. Rev. B **38**, 1573 (1988); D. C. Rodenberger and A. F. Garito, Nature **359**, 309 (1992).

[2] S. Etemad and Z. G. Soos, in *Spectroscopy of Advanced Material*, edited by R. G. Clark and R. E. Hester (Wiley, New York, 1991), pp. 87–133, and references therein.

[3] *Nonlinear Optical Properties of Organic Molecules and Crystals*, edited by J. Zyss and D. S. Chemla (Academic, Florida, 1987), Vols. 1, 2.

[4] A. Takahashi and S. Mukamel, J. Chem. Phys. **100**, 2366 (1994); S. Mukamel, A. Takahashi, H. X. Wang, and G. Chen, Science **266**, 251 (1994).

[5] C. Bubeck, in *Nonlinear Optical Material: Principles and Applications*, edited by V. Degiorgio and C. Flytzanis (IOS Press, Amsterdam 1995), p. 359.

[6] S. Mukamel, *Principles of Nonlinear Optical Spectroscopy* (Oxford, New York, 1995).

[7] W. E. Torruelas, D. Neher, R. Zanoni, G. I. Stegeman, and F. Kajzar, Chem. Phys. Lett. **175**, 11 (1990); M. Cha, W. E. Torruelas, G. I. Stege-

man, N. X. Wang, A. Takahashi, and S. Mukamel, *ibid.* **228**, 73 (1994).
[8] W. J. Buma, B. E. Kohler, and T. A. Schuler, J. Chem. Phys. **96**, 399 (1992).
[9] A. Mathy, K. Ueberhofen, R. Schenk, R. Garay, K. Millen, and C. Bubeck, Phys. Rev. B **53**, 4367 (1996).
[10] G. P. Agrawal, C. Cojan, and C. Flytzanis, Phys. Rev. B **17**, 776 (1978).
[11] Z. Shuai and J. L. Brédas, Phys. Rev. B **44**, 5962 (1991); D. Beljonne, Z. Shuai, and J. L. Brédas, J. Chem. Phys. **98**, 8819 (1993).
[12] F. S. Spano and Z. G. Soos, J. Chem. Phys. **99**, 9265 (1993).
[13] I. D. W. Samuel, I. Ledoux, C. Dhenaut, J. Zyss, H. H. Fox, R. R. Schrock, and R. J. Silbey, Science **265**, 1070 (1994).
[14] M. Blanchard-Desce, J. M. Lehn, M. Barzoukas, I. Ledoux, and J. Zoss, J. Chem. Phys. **181**, 281 (1994).
[15] J. P. Hermann and J. Ducuing, J. Appl. Phys. **45**, 5100 (1974).
[16] H. Kuhn, Fortschr. Chem. Org. Naturstoffe **17**, 404 (1959).
[17] E. F. McIntyre and H. F. Hameka, J. Chem. Phys. **68**, 3481 (1978); D. N. Beratan, J. N. Onuchic, and J. W. Perry, *ibid.* **91**, 2696 (1987).
[18] S. Mukamel and H. X. Wang, Phys. Rev. Lett. **69**, 65 (1992).
[19] B. M. Pierce, Physica D **68**, 51 (1993).
[20] G. S. W. Graig, R. E. Cohen, R. R. Schrock, C. Dhenaut, I. LeDoux, and J. Zyss, Macromolecules **27**, 1875 (1994).
[21] C. Flytzanis and J. Huttler, in *Contemporary Nonlinear Optics*, edited by G. P. Agrawal and R. W. Boyd (Academic, San Diego, 1992), pp. 297–365.
[22] D. Neher, A. Kaltbeitzel, A. Wolf, C. Bubeck, and G. Wegner, in *Conjugated Polymeric Materials: Opportunities in Electronics, Optoelectronics and Molecular Electronics*, edited by J. L. Brédas and R. R. Chance (NATO ASI E 182, Kluwer, Dordrecht, 1990).
[23] J. L. Bredas, C. Adant, P. Tackyx, A. Persoons, and B. M. Pierce, Chem. Rev. **94**, 243 (1994).
[24] V. Chernyak and S. Mukamel, J. Chem. Phys. **104**, 444 (1996).
[25] P. Ring and P. Schuck, *The Nuclear Many-Body Problem* (Springer-Verlag, New York, 1976).
[26] H. Sekino and R. J. Bartlett, J. Chem. Phys. **98**, 3022 (1993).
[27] R. McWeeny and B. T. Sutcliffe, *Methods of Molecular Quantum Mechanics* (Academic, New York, 1976).
[28] V. Chernyak and S. Mukamel, J. Chem. Phys. **103**, 7640 (1995).
[29] J. K. Cullum and R. A. Willoughby, J. Comp. Phys. **44**, 329 (1981); T. J. Park and J. C. Light, J. Chem. Phys. **85**, 10 (1986); C. Leforestier, R. H. Bisseling, C. Cerjan, M. D. Feit, R. Friesner, A. Guldberg, A. Hammerich, G. Jolicard, W. Karrlein, H.-D. Meyer, N. Lipkin, O. Roncero, and R. Kosloff, J. Comp. Phys. **94**, 59 (1991).
[30] H. Mori, Prog. Theoret. Phys. **33**, 423; **34**, 399 (1965); R. Zwanzig, Lect. Theoret. Phys. **3**, 106 (1961).
[31] G. Brosso and G. Pastori Parravicini, Adv. Chem. Phys. **62**, 81 (1985); **62**, 133 (1985).
[32] R. R. Ernst, G. Bodenhausen, and A. Wokaun, *Principles of Nuclear Magnetic Resonance in One and Two Dimensions* (Clarendon, London, 1987).
[33] H. Fukutome, J. Mol. Struct. (Theochem) **188**, 337 (1989), and references therein.
[34] M. Hartmann, V. Chernyak, and S. Mukamel, Phys. Rev. B **52**, 2528 (1995).
[35] B. Kirtman, J. L. Toto, K. A. Robins, and M. Hasan, J. Chem. Phys. **102**, 13 (1995); T. T. Toto, J. L. Toto, C. P. de Melo, M. Hasan, and B. Kirtman, Chem. Phys. Lett. **244**, 59 (1995).
[36] S. Tretiak, V. Chernyak, and S. Mukamel (unpublished).
[37] D. S. Chemla and J. Y. Bigot, Chem. Phys. (1996) (in press); D. S. Chemla, J. Y. Bigot, M. A. Mycek, S. Weiss, W. Schafer, Phys. Rev. **50**, 8439 (1994-II).
[38] L. Bányai and S. W. Koch, *Series on Atomic, Molecular and Optical Physics* (World Scientific, Singapore, 1993), Vol. 2.
[39] L. E. Brus, J. Chem. Phys. **80**, 4403 (1984).
[40] A. A. Kirillov, *Elements of the Theory of Representations* (Springer, Berlin, 1976).
[41] G. A. Korn and T. M. Korn, *Mathematical Handbook* (McGraw-Hill, 1968).
[42] G. H. Golub and C. F. Van Loan, *Matrix Computation* (Johns Hopkins University Press, Baltimore, MD, 1983).
[43] B. E. Kohler, C. Spangler, and C. Westerfield, J. Chem. Phys. **89**, 5422 (1988); I. Ohmine and M. Kaplus, *ibid.* **68**, 2298 (1978).